SAE INTERNATIONAL AERO DESIGN CHALLENGE EAST - 2022

MICRO CLASS DESIGN REPORT

By

TEAM NUMBER : 312
TEAM NAME: IARE LAKSHYA

TEAM MEMBERS:

L V S S Lohitasya Varun (Captain)	Apoorva Jammalamadaka
Pranav Tej Gurram	Niharika Pothuri
N Lakshmi Narasimhan	K Barghava Ramudu
Sumanth Pasumarthi	Kammari Vamshi Krishna
Venkatesh Daripalli	Vishnu Vardhan Gottala
Jayendra Rajanala	Saksham Gedam
Vemula Manasa	Mukarram Hussain

Table of Contents

1 Introduction

Current technological breakthroughs have encouraged digitization across a variety of industries, resulting in successful connections between suppliers and consumers across many locations. This has necessitated the development of a product that is both ecologically friendly and quick. The fundamental job of a team is to plan and construct a model with fresh ideas and surprises. On a single stretch, designing an unmanned vehicle with enhanced structure, flight performance, aerodynamics, and avionics is a difficult task. A certain design can be established as the final design after several attempts and failures, the same process has been applied to the present problem statement for a successful design output.

1.1 Mission Profile:

The entire mission profile for the SAE International Micro class event is described in the image shown below:
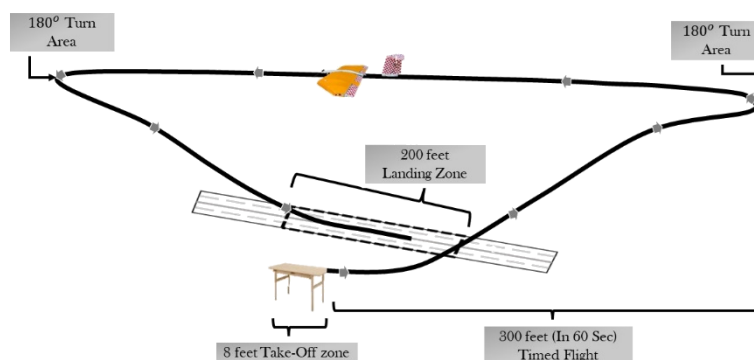
Figure 1: Mission Profile

2 Problem Statement

The team decided to design an aircraft abiding all the rules and regulations given by SAE International. The ultimatum was to assimilate the design constraints posed with cruising at a moderately high altitude.

2.1 Design Requirements and Constraints

Table 1: Design Requirements for Mission

S.no	Design Feature	Constraint or Requirement
1	Take-off distance	8 feet
2	Landing Distance	200 feet
3	Timed distance	300 feet
4	Minimum Speed	5 ft/s
5	Maximum wing span	48 inches
6	Propulsion Type	Electric
7	Powerplant	Maximum of 4 cells Li-Po
8	Power Limit	450 Watts

3   Design Selection and Review Process

3.1   Background and Scoring Strategy

The mission profile dictates that the aircraft needs to be STOL capable, taking-off from 2 ft elevated platform of 8 ft length whilst carrying a payload and delivery boxes. Hence the work began by calculating the maximum number of boxes that could be carried without causing too much of a hassle in making the design aerodynamic. The number of different combinations of small and large boxes to points scored, was analyzed and the most optimal solution was found to be carrying <u>2 large payload delivery boxes,</u> which was both aerodynamically feasible and fetched a better overall flight score. The above conclusions were deduced from the following pareto graphs where L and S refers to large and small payload delivery boxes mentioned in the X axis.

Graph 1: Weight (lb) vs Combination of Boxes

Graph 2: Volume (cu.in) vs Combination of Boxes

Graph 3: Bonus Points vs Combination of Boxes
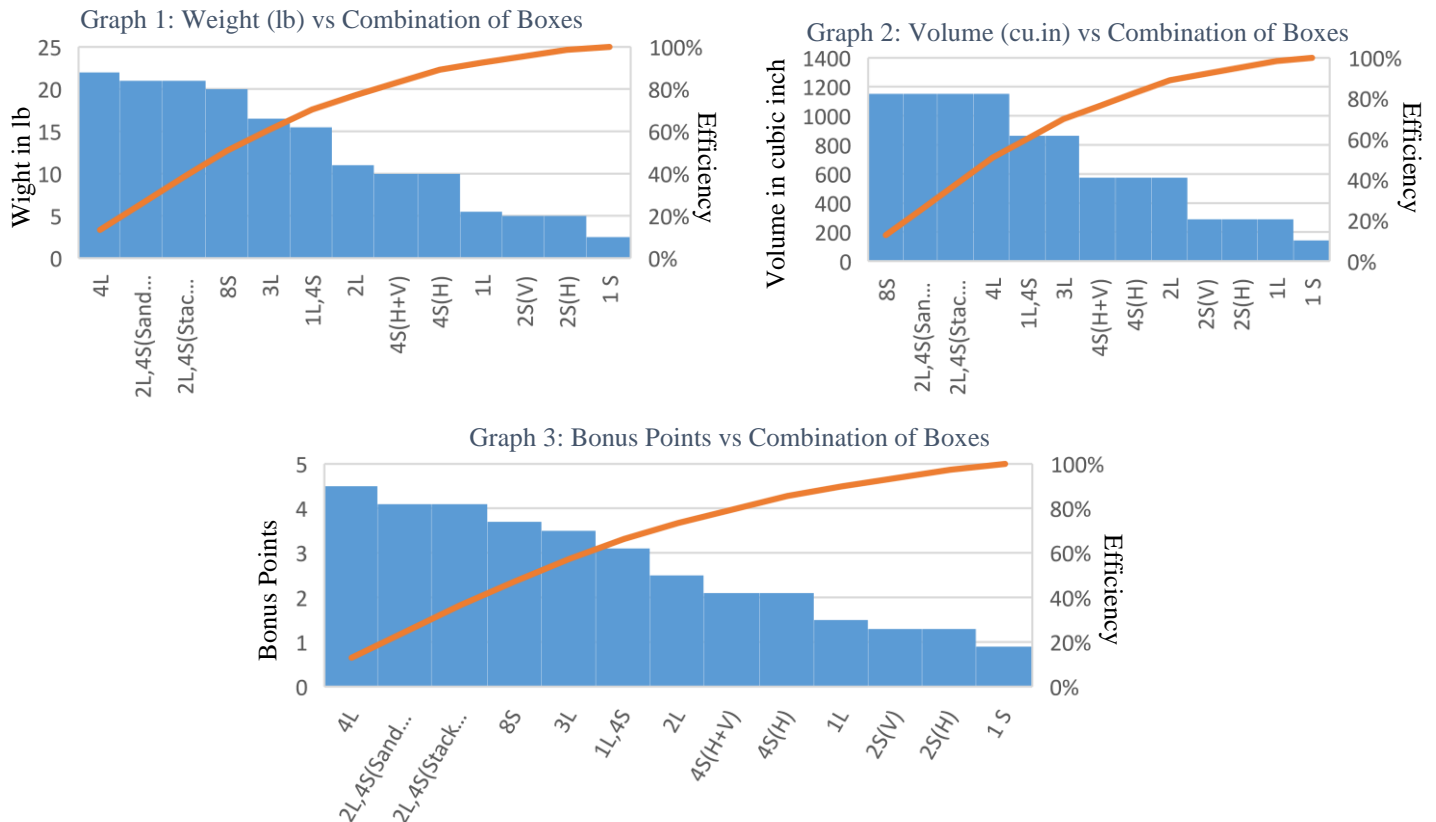
The design has meticulously undergone a series of iteration and immaculate thought processes to conclude with the current configuration. The overlaps of which are shown below for an idea. The analysis of all these models were initially done computationally to save material and budgetary costs, although the last few iterations were experimentally tested as well to tally the virtual simulations done so far. The iterations overlap clearly shows the chain of thought, of the team towards the end of the design
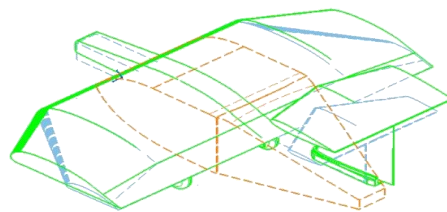

Figure 2: Iterations Overlap

3.2   Literature Review

Cargo Planes

➢ Tend to have a wider area of cross section.

➢ High wing configuration to allow the payload to be nearer to the ground.

➢ High mounted tail section for the ease of payload loading and unloading.

STOL

➢ They tend to have a high power to weight ratio at the time of take-off.

➢ They have a back drop of maximum speed.

➢ They are designed for low endurance missions.

➢ Have large wings and high lifting devices like flap, slots, slats and vortex generators.

➢ Provide better flexibility while landing in various terrains.

Small Aspect Ratio Planes

➢ Tend to have higher chord or lower wing area as per formula

➢ The thrust required to go airborne is typically high, due to less area to produce required lift.

➢ It helps in decreasing zero-lift drag.

➢ Smaller AR helps in having a lower wing weight (Structural).

➢ Sweep angle also provides lower AR while keeping area constant for higher speeds.

High T Tail

➢ Provide low disturbance on the tail due to wing's downwash.

➢ Helps aircraft gain control during spin.

➢ Less pitch control effectiveness.

➢ Reduces air pressure losses.

➢ Interference of rudder is removed.

➢ Increases cargo clearance.

➢ Undergo stall at higher angle of attack.

➢ Needs stronger vertical stabilizers, so possibly tail heavy.

➢ Provides propulsion system at rear end of fuselage as interference on tail is less.

➢ Mostly used to for heavy cargo aircrafts.

3.3 Trade-off Studies

The following trade-offs were made by using previously generated data and thorough simulation for maximum possible efficiency for present scenario. (The green shaded rows/columns indicate selected configuration based on total score). The score factor has been decided based on the influence of that particular design feature on the entire model.

3.3.1 Wing Configuration Selection

Table 2: Wing Trade-Off

Type	Figure of Merit	L/D	Stability	Structural Weight	Compactness	Ease of Manufacture	Total Score
	Score Factor	0.4	0.2	0.1	0.2	0.1	
Wing Structure	Anhedral	1	1	0	0	1	0.8
	Dihedral	0	1	1	1	1	0.6
	Zero Angle	1	1	1	1	0	0.9
	Flying Wing	1	1	0	0	0	0.6
	Delta	0	1	1	1	0	0.5
Wing Planform	Swept	0	1	0	1	0	0.8
	Tapered	1	1	1	1	0	0.9
	Rectangle	1	1	0	0	1	0.3
Wing Positioning	High	1	1	1	NA	0	0.7
	Middle	1	0	1	NA	0	0.7
	Low	0	1	0	NA	1	0.3

The wing was therefore chosen to be a rectangular till the delivery box and taper from thereafter without having any dihedral or anhedral to ease the manufacturing process and retain structural strength as per the structural limits for materials selected in the section 3.4 .

3.3.2 Fuselage, Tail and Motor Configuration Selection

Table 3: Tail , Fuselage and Motor Configuration

	Figure of Merit	Score factor	Conventional	V-tail	T - Tail
Tail configuration ranking	**Stability**	0.3	0	0	1
	Drag	0.2	1	0	1
	Structural Weight	0.4	1	0	0
	Manufacturability	0.1	1	0	1
	Total Score		0.7	0.2	0.6
Fuselage configuration ranking			**Conventional and Embedded in Wing**	**Single Boom**	**Twin Boom**
	Weight Distribution	0.4	1	1	0
	Stability	0.2	1	0	0
	Structural Weight	0.3	0	1	1
	Manufacturability	0.1	1	0	1
	Total Score		0.7	0.7	0.4
Motor configuration ranking			**Pusher**	**Push- Pull Motor**	**Tractor**
	Weight	0.2	1	0	0
	Power	0.3	0	1	1
	Efficiency	0.3	1	0	1
	Thrust Factor	0.2	1	0	1
	Total Score		0.7	0.3	0.8

3.4 Overall Configuration:

Table 4: Final Configuration Selection

Wing	Rectangular and tapered at tips, with no angle of dihedral mounted in the middle
Fuselage	Cubically aerodynamic fuselage with weight reduction holed while embedded in wing
Tail	Single Fin, T-tail
Motor	Single tractor with fuselage centred

3.5   Material Selection:

Table 5: Materials Properties

S. No	Material	Properties	Advantages	Locations of Usage
1.	**Carbon Fibre 3K Crosshatch rolls (Prepreg)**	High strength and shock absorbing	Lightweight, Reduces Flow separation, easy to mend into shapes	Spars of wing, horizontal tail and fin
2.	**ABS Plastic (3D Printed)**	Anti-corrosive and has high yield strength. Thermoset material.	Ease of designing and shaping	Fuselage - Boom Clamp and Tail Mount
3.	**Aircraft Grade Aluminium (AA6061)**	Alloy of Titanium and Aluminium	Provides overall structural strength to framework	Nose and main Landing Gears
4.	**Balsa Wood**	Low density, light weight and rigid	Light weight and highly brittle to retain shape	Wing and Tail Ribs, Fuselage body
5.	**Aeroply**	Light weight, high flexural rigidity in woods	High strength to weight ratio in woods, resistance to bending	Wing and Tail Ribs
6.	**Acrylic Sheet**	High plasticity, outstanding strength, stiffness, and optical clarity.	Heat mouldable into desired shapes, crash resistant and readily available	Wing Leading edge

The materials have been chosen taking into account, the various stresses and strains the particular component would face and thus arriving at a conclusion by using ANSYS GRANTA Module for apt material selection. The ANSYS GRANTA was also used to analyse the materials to help finish final sorting of the materials. [24]

4 Commercially Off the Shelf Components (COTS)

4.1 Powerplant Configuration

Table 6: Motor Selection

Motor	T-Motor AT2820	SunnySky X2820 V3	Emax MT3515
KV	880	860	650
Weight (lb)	0.306	0.315	0.288
Rated Voltage (Lipo)	3-4S	3-4S	4-6S
Peak Current (A)	45	65	36
Idle Current (A)	1.6	1.3	1.7
Rotor Diameter	35.2	35	41.5
Body Length	1.771	1.653	1.314
Cost (USD)	59.99	35	29.7

Motor	T-Motor AT2820				SunnySky X2820 V3				Emax MT3515			
Propeller	Dual Blade 12*6				Dual Blade 13*8				Dual Blade 14*4.7			
Throttle (%)	40	60	80	100	40	60	80	100	40	60	80	100
Thrust (lb)	2.08	3.17	4.92	6.07	1.65	2.76	3.86	4.96	1.65	2.71	3.64	4.74
Voltage (V)	15.15	15.03	14.80	14.59	11.10	11.10	11.10	11.10	14.80	14.80	14.80	14.80
Current (A)	8.88	15.95	29.60	42.00	8.00	18.20	30.00	43.30	6.00	12.00	20.00	29.30
Power (W)	134.4	239.7	438.0	612.7	88.8	202.0	333.0	480.6	88.8	177.6	296.0	433.6
Efficiency (lb/W)	14.48	6.00	5.09	4.50	19.71	6.19	5.26	4.68	19.71	6.93	5.57	4.96
Preference	High				Moderate				Low			

The **motor will be constrained** via the transmitter to go only up to **80% of the throttle** to avoid loss of power from the SAE Power limiter which limits power above 450 W.

4.1.1 ESC selection

Table 7: ESC Selection

ESC	T-Motors AT 55A	Hobbywing Skywaller 50A	Phoenix Edge Lite 50A
Continuous Current (A)	55	50	50
Peak Current(10s) (A)	75	65	60
Weight (g)	0.139	0.090	0.123
Lipo	2-6S	2-4S	2-8S
Size/L*W*H (in)	3.031*1.378*0.551	2.56*1.378*0.551	2*1*0.913
Cost (USD)	29.99	26	94.95

4.1.2 Battery Selection

Table 8: Battery Selection

Battery	Bonka	Lumenier	Orange
Capacity (Ah)	1.5	1.5	1.5
Voltage (V)	14.8	14.8	14.8
Max Continuous Discharge ©	45	75	100
Max Burst Discharge ©	90	150	200
Weight (lb)	0.342	0.373	0.430
Capacity/Weight	4.39	4.02	3.49
Size (L*W*H) (in)	2.756*1.300*1.181	2.952*1.338*1.338	2.952*1.300*1.338
Cost (USD)	34.49	31.99	31.13

4.1.3 Propeller Selection

Table 9: Propeller Selection

Propeller	APC 12*6	APC 13*8	APC 14*4.7
Type	Dual-Blade fixed	Dual-Blade fixed	Dual-Blade fixed
Diameter (in)	12	13	14
Pitch (in)	6	8	4.7
Weight (lb)	0.101	0.108	0.055
Hub Diameter (in)	1	1	0.5
Hub Thickness (in)	0.48	0.48	0.3
Shaft Diameter (in)	0.25	0.25	0.25
Cost (USD)	5.13	6.9	6.21

The motor, ESC, battery and propeller selected are shown as highlighted green columns.

5 Static and Dynamic Thrust Calculation

Table 10: Static and Dynamic Thrust

Throttle %	Power (W)	Speed (m/s)					
		10	9	8	7	6	0 (Static Thrust)
		Speed (ft/s)					
		32.81	29.53	26.25	22.97	19.69	0.00
40	134.43	1.6144	1.6615	1.7086	1.7557	1.8028	2.0854
50	185.48	2.0994	2.1526	2.2059	2.2592	2.3125	2.6321
60	239.66	2.5971	2.6542	2.7113	2.7684	2.8255	3.1680
70	326.02	3.3304	3.3928	3.4552	3.5176	3.5800	3.9545
80	438.01	4.2650	4.3303	4.3955	4.4607	4.5260	4.9175
90	555.43	5.0231	5.0933	5.1634	5.2335	5.3036	5.7243
100	612.71	5.3616	5.4330	5.5044	5.5758	5.6471	6.0753

The Total static thrust that can be generated by the motor at 100% throttle is 6.0753 lbs, but the power consumption at this throttle percent is 612.71 W. Since we have a power limiter of 450 W, we intend to operate the motor at 80% throttle, thereby giving us a maximum static thrust of 4.9175 lbs, while consuming 438.01 W of power. The dynamic thrusts at different throttle percentages and speeds are shown in the table above

The **motor will be constrained** via the transmitter to go only up to **80% of the throttle** to avoid loss of power from the SAE Power limiter

6 Power Source Calculation

The power limitation of 450 Watts has constrained us to assume the maximum power usage during the entire flight and proceed with the battery selection.

The simple formulae that $\underline{P = V \times I}$ was used to obtain the current . Since P = 450 W and the V= 14.8V (since 4S LiPo is used), we find the continuous Amperage draw to be 30.4 A.

Since the assumed flight time to complete the mission profile is less than or equal to a minute, a 4 cell LiPo battery with 500 mAh capacity should be able to provide sufficient power for the entire course of flight. In order to make sure the battery had enough power to overcome any external forces such as gusts and other losses due to environmental conditions and usage such as pre-flight checks, a 4 cell LiPo battery with a capacity of 1500 mAh was chosen which can provide us the required continuous current for a period of about 3 minutes in ideal conditions.

6.1.1 Avionics Weight Buildup

Table 11: Avionics Weight Buildup

S.No	Components	Weight
1	Battery	0.341
2	Motor	0.306
3	ESC	0.139
4	Propeller	0.101
5	Servos	0.172
6	Receiver	0.033
7	Miscellaneous wires and connectors	0.661
TOTAL		**1.753**

6.2 Airfoil Selection

Initially a lot of conventional low drag airfoils were selected to be implemented for the wing but upon design iterations, none of the airfoils had the required design feature to accommodate the delivery boxes inside them. Hence a custom designed airfoil was finally chosen among other airfoils which was showing promising results to suit our payload carrying needs.
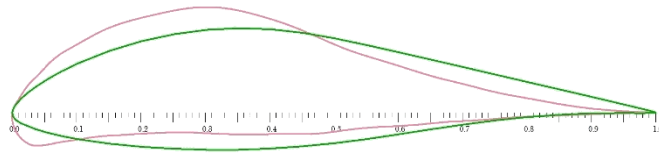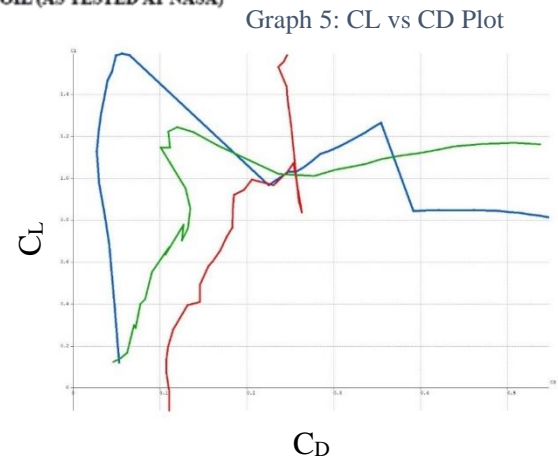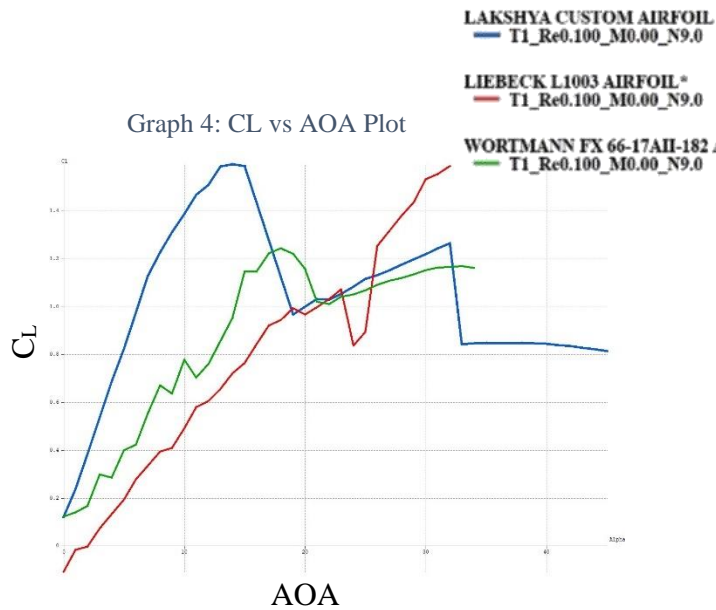

Figure 3: Other Considerable Airfoils
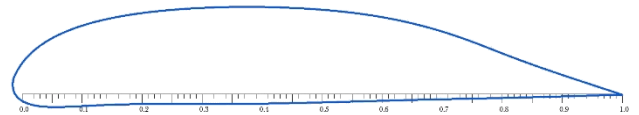
Figure 4: Custom Designed Airfoil

LAKSHYA CUSTOM AIRFOIL
— T1_Re0.100_M0.00_N9.0

LIEBECK L1003 AIRFOIL*
— T1_Re0.100_M0.00_N9.0

WORTMANN FX 66-17AII-182 AIRFOIL (AS TESTED AT NASA)
— T1_Re0.100_M0.00_N9.0

Graph 4: CL vs AOA Plot

C_L

AOA

Graph 5: CL vs CD Plot

C_L

C_D

7 Weight Estimation

The entire weight of the aircraft is estimated using prototype values and simple calculations as follows:

Table 12: Weight Estimation

S.No.	Component Name	Weight(grams)	Weight(lb)
1	Propeller	45.926	0.101
2	Motor	139.000	0.306
3	Boom	76.000	0.168
4	Tail mount	123.200	0.272
5	Fin	92.050	0.203
6	Fuselage	270.400	0.596
7	Tail	170.350	0.375
8	Wing	701.400	1.546
9	Landing gear	495.000	1.090
10	Payload	453.000	1.000
11	Battery	155.000	0.342
12	Delivery Box-port	170.000	0.375
13	Delivery Box-starboard	170.000	0.375
14	Landing gear servo	13.400	0.030
15	Aileron servo - port	13.400	0.030
16	Aileron servo - starboard	13.400	0.030
17	Flap servo - port	13.400	0.030
18	Flap servo - starboard	13.400	0.030
19	Elevator servo	13.400	0.030
20	Rudder servo	13.400	0.030
21	ESC	63.000	0.139
22	Power Limiter	18.000	0.040
23	Receiver	14.900	0.033
24	Miscellaneous (adhesives, connectors, fasteners, etc)	350.000	0.772
	TOTAL	**3601.026**	**7.939**

8   Aircraft Sizing

8.1.1   Wing, Rib and Spar Sizing

The wing sizing has been done taking Mission Requirements into consideration and extrapolating them to meet the needs of aircraft design. The wing planform has been designed according to cargo carrying UAV requirements, but the span limitation made the deciding of wing planform slightly tougher. Hence, the payload delivery boxes were decided to be inserted in the wing through the leading edge so as to not lose any amount of lift due to external mounting of the boxes during cruise and also to increase range and endurance. (Iqbal et al., 2008)

The aircraft wing was fixed to be tapered after the rectangular section with total span of 47 inches, taper ratio of 1.29 and an aspect ratio of 2.234. A large surface for Fin is given for added lateral stability. The ribs were optimized using Wing Helper to reduce the weight without compromising structural integrity. (Panagiotou et al., 2016)

The ribs and spars were sized accordingly and analyzed for their structural capability to withhold the payload delivery boxes and at the same time posses the minimum weight possible.
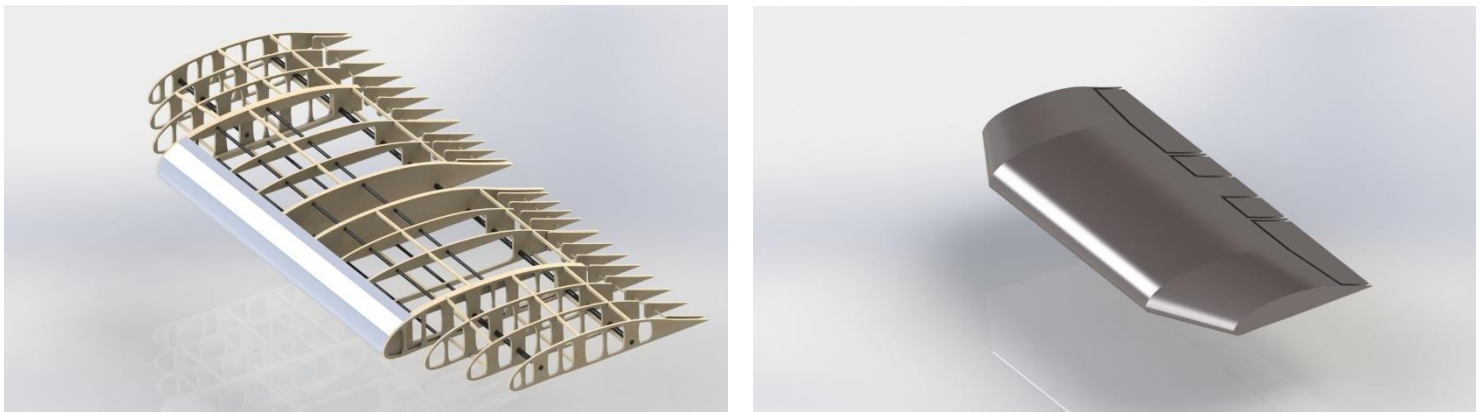
Figure 5: Wing Rib Structure and Solid View Render

Table 13: Wing Sizing

Parameter	Main Wing
Wing Span	47 inches
Wing Surface Area	989 in^2
Aspect Ratio	12.607
Root Chord	22 inches
Taper Ratio	1.294
Sweep Angle	9.07^0
MAC	21.151 inches

8.1.2 Fuselage Sizing

The fuselage, as previously mentioned has been carefully attempted to be embedded in the wing to avoid interference from the high or low mounted wings as they had a tendency to swirl the flow at the roots of the wing much more than currently applied design. Owing to constraints of the main wing and empennage, the fuselage has been sized to a length of 29 in (from nose to wing TE) and a width of 3.3989 in. The distance from nose of the aircraft to the leading edge of tail was fixed to be 47 in from for a higher static stability giving the tail arm length of 21.262 in.

Figure 6: Fuselage Iso View render

8.2 Empennage Sizing

The Empennage for the aircraft was initially thought to be a conventional tail at the same datum level as the wing. But the enormous wing surface area created a large downwash which led the tail to be in the wake of the wing and hence the T-tail configuration was finally chosen with the structure as shown below:
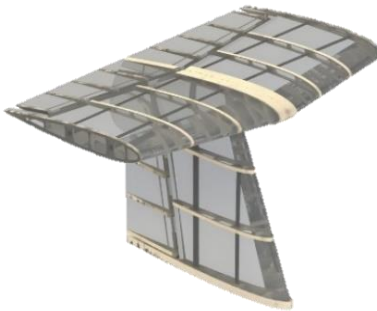
Figure 7: Empennage Iso View Render

8.2.1 Horizontal Tail

Table 14: Horizontal Tail

Specifications	Dimensions
Span	18 inches
Surface area	198 in^2
Aspect ratio	1.64
Taper ratio	1.20
Root chord	12 inches
Mean Aerodynamic Chord	11.03 inches
Sweep angle	9.46^0

8.2.2 Vertical Tail

Table 15: Vertical Tail Sizing

Specifications	Dimensions
Span	20 inches
Surface area	100 in^2
Aspect ratio	2.00
Taper ratio	1.50
Root chord	12 inches
Mean Aerodynamic Chord	10.13 inches
Sweep angle	16.70^0

The sizing for the horizontal and vertical tails were calculated using sizing thumb rules from Daniel P Raymer's Book "Aircraft Design" and adjusted accordingly in the XFLR5 software.

8.3 Control Surface Sizing

The primary control surfaces are used to maneuver the aircraft according to the flight plan and adjust to its intended flight path.

8.3.1 Aileron and Flaps Sizing

The aileron is a primary control surface used to provide the rolling moment and are placed on the Trailing edge of the wing to give maximum moments during cruise. The ailerons were sized using the formula by Mohammad Sadraey.

They were sized and placed into the wing without changing the chord of the wing.

Thus, the final aileron dimensions were 4.4in at root and 3.4in at tip with span of 14.1in on each side with thickness made to match the airfoil of the wing at that location.

8.3.2   Rudder and Elevator Sizing

The rudder and elevator were sized based on the equations again adapted from the book "Aircraft Design: A Systems Engineering Approach by Md Sadraey". The formulated rudder and Elevator dimensions were:

Elevator: 0.09 m x 0.72m (on each side of elevator)

Rudder: 0.36 m x 0.13 m

8.3.3   Servo Sizing

The servos play an important in operating the control surfaces and providing the necessary torque to maneuver the aircraft using the moments so produced. The empirical formula between the torque required and the control surface area is given by:

$$T = 8.5 * 10^{-6} * \frac{c^2 * v^2 * l * \sin(S_1) * \tan(S_1)}{\tan(S_2)}$$

$T \rightarrow$ Torque in Nm
$v \rightarrow$ Velocity of aircraft in kmph
$c \rightarrow$ Chord length of the control surface in m

$l \rightarrow$ Length of the control surface in m
$S_1 \rightarrow$ Maximum control surface deflection
$S_2 \rightarrow$ Maximum servo angle deflection

Hence the torque required by the servos for different control surfaces are as follows in imperial units:

Table 16: Control Surface Torque Prediction

S. No	Control Surface	Servo Torque Needed
1	Aileron	91.60 e-7 lb-in
2	Flaps	53.76 e-7 lb-in
3	Rudder	36.02 e-7 lb-in
4	Elevator	73.1 e-7 lb-in

9   Environmental Conditions and Assumptions

Table 17: Environmental Conditions Assumptions

S. No	Parameter	Assumed Value
1	Air Density	0.0765 lb/ft^3
2	Atmospheric Pressure	14.69 PSI
3	Altitude	300 ft
4	Temperature	59^{0}F
5	Gust Load (from Avg Wind Speed)	0.002642 PSI

The altitude of the aircraft in this case is limited by the range of the transmitter. The temperature, gust load and pressure are taken from Fort Worth average weather using online data.

10 Design Analysis

The entire design has been carefully analyzed in all the aspects to deem the aircraft flight worthy through the computational simulations run in **XFLR5, MATLAB** and **ANSYS** with all the real time conditions faced by the aircraft during the course of its flight.

10.1 Airfoil Analysis

As mentioned earlier the custom designed airfoil was analyzed through multiple iterations to achieve the desired results as well as accommodate the delivery boxes. The following is the airfoil pressure data obtained through **MATLAB** simulation of the airfoil.

Graph 6: Airfoil Pressure Distribution Plot
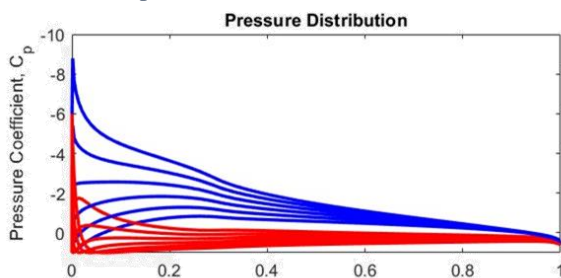
10.2 Lift, Drag and Moment Prediction

The lift and drag have been analyzed from both **MATLAB** and **XFLR5** to tally the results computationally and therefore validate our results.


```
IARE LAKSHYA
Wing Span      =    47.000 in
xyProj. Span   =    47.000 in
Wing Area      =   989.000 in²
xyProj. Area   =   989.000 in²
Plane Mass     =     7.947 lb
Wing Load      =     0.008 lb/in²
Tail Volume    =     0.241
Root Chord     =    22.000 in
MAC            =    21.151 in
TipTwist       =     0.000°
Aspect Ratio   =     2.234
Taper Ratio    =     1.294
Root-Tip Sweep =     9.067°
XNP = d(XCp.Cl)/dCl =   8.929 in
Mesh elements  = 1981
```
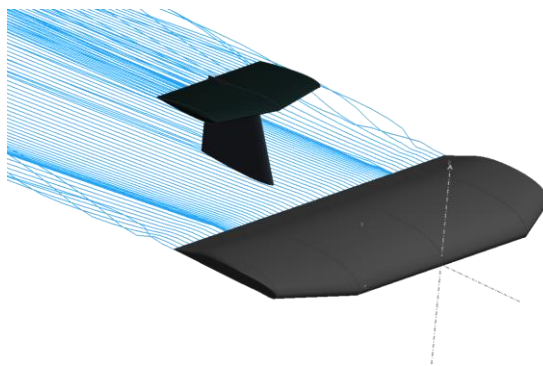
```
        V =   26.2 ft/s
    Alpha =    0.000°
     Beta =    0.000°
       CL =    0.252
       CD =    0.009
Efficiency =   1.009
    CL/CD =   28.158
       Cm =   -0.024
       Cl =    0.000
       Cn =    0.000
     X_CP =   12.282 in
     X_CG =   10.265 in
```

Figure 8: XFLR5 Analysis Result

Table 18: Analytical vs Computational Results Comparison

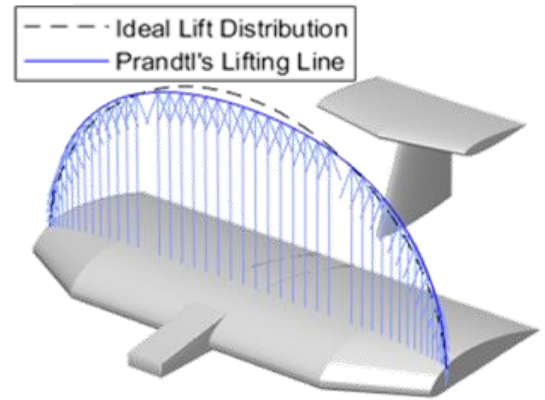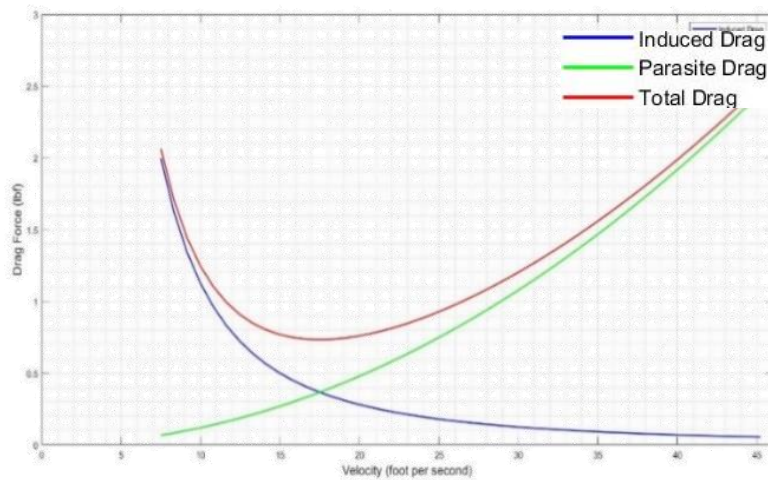| S.No	Aerodynamic Parameter	Analytical Result (MATLAB)	Computational Result (ANSYS)
1	Lift	1.3786 lbf	1.8627 lbf
2	Drag	0.2406 lbf	0.2484 lbf
3	L/D	5.7298	7.498

Graph 7: Drag Polar

Figure 9: Prandtl's Elliptical Lift Distribution

The above depicted drag polar can be expressed as: $C_D = 0.034 + 0.1566\ CL2$, where

Parasitic drag = C_{D0} = 0.034 and induced drag parameter (k) = $1/(\pi \times e \times AR)$ = 0.1566
AR → Aspect ratio; e→ Oswald's Efficiency factor
Oswald's efficiency factor (e) was calculated using the empirical formula derived from various experimental work which is as follows:
e = $1/(1.05+0.007 \times \pi \times AR)$, this formula gave e = 0.9098 for our wing

10.3 Aircraft Stability and Control Analysis

The stability and controllability of the aircraft is a crucial aspect in deeming the aircraft flight worthy, without a proper controllable aircraft the entire mission is rendered moot. The stability is the ability of the aircraft to overcome adverse aerodynamics forces during the course of its flight and remain steadfast in the designated flight path. This analysis has been thoroughly analyzed using the XFLR5 software and by plotting all the time response graphs as required.

10.3.1 Lateral Dynamic Stability

The Lateral Dynamic Stability of aircraft defines its's ability to recover from a laterally directed disturbance and the ability to return to its stable position without compromising the manoeuvrability. The below graph trend of the aircraft's lateral stability time response shows a steep dampening line depicting the high lateral stability of the aircraft.

Graph 8: Longitudinal Dynamic Stability Time Response
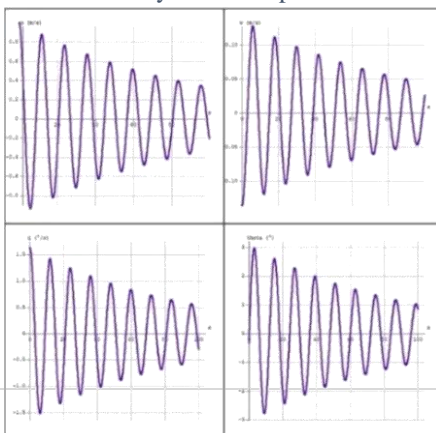
Graph 9: Lateral Dynamic Stability Time Response
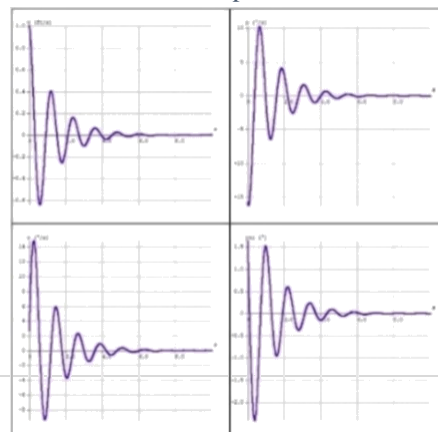
10.3.2 Longitudinal Dynamic Stability

Similar to the lateral dynamic stability, the longitudinal dynamic stability plots have been recorded using the same procedure and the resulting graphs have been studied to have been found that the aircraft is in fact longitudinally stable as well. The graphs above show that the aircraft takes about 80 seconds to dampen the gust force amplitude, in a ratio that does not compromise longitudinal maneuverability by dampening the oscillations too intense or too slow.

10.4 Flow Analysis

The Computational Fluid Dynamic Analysis was performed in ANSYS 19.2 using 101 million mesh elements to capture the detailed characteristics of the flow field around the aircraft as it proceeds through air. The settings used and the contours obtained thereof are as follows:

Table 19: Flow Analysis Parameters

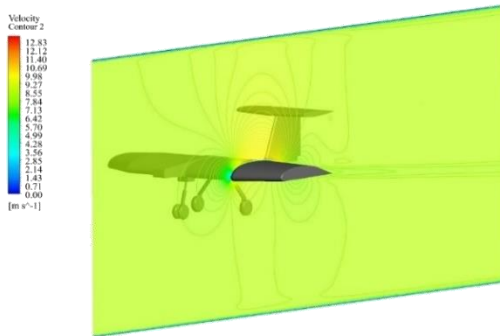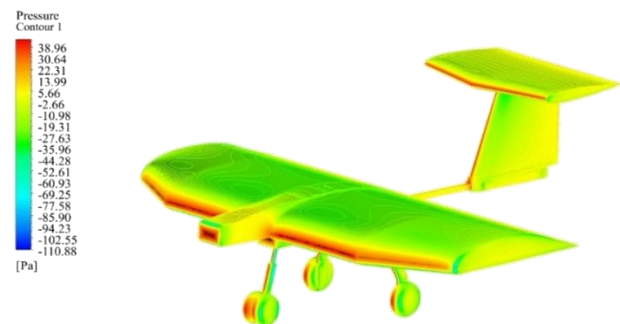| S. No	Parameter	Value	Imperial Unit value
1	Mesh Element Size	10 mm	0.394 in
2	Proximity Capture Sizing	0.01mm	0.000394 in
3	Curvature Capture Sizing	0.01 mm	0.000394 in
4	Inlet Velocity	8 ms^{-1}	26.247 ft/s
5	Outlet Pressure	0 Pa	0 PSI
6	Walls Condition	No Slip	-
7	Solver Scheme	SIMPLE	-
8	Convergence Criteria	Achieved	-

Figure 10: Velocity Contour Iso view

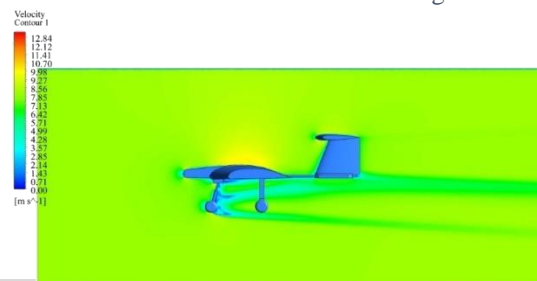Figure 11:Surface Pressure Contours

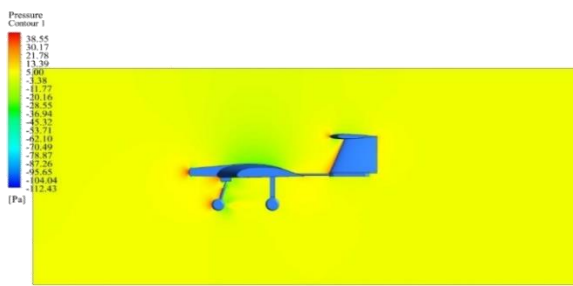Figure 12: Velocity Contour Side View
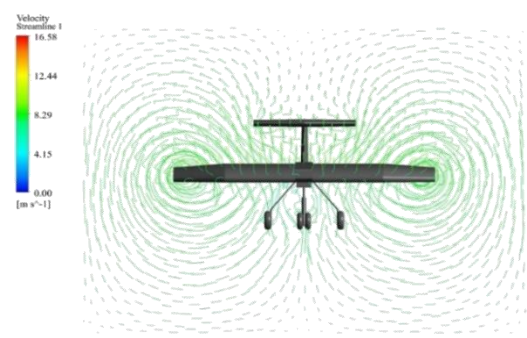
Figure 13: Pressure Contours Side view

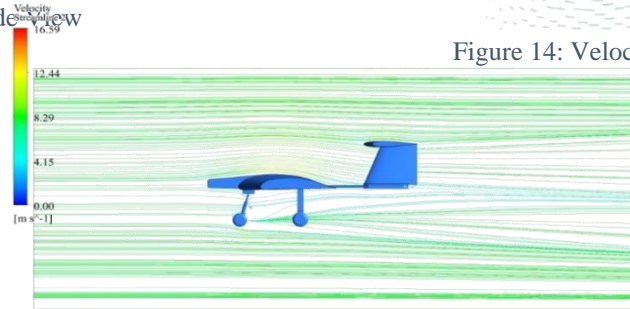Figure 14: Velocity Streamlines Front View

Figure 15: Velocity Streamlines Side view

10.5 Structural Analysis

The structural analysis too was performed in ANSYS 19.2 Mechanical APDL Solver using the structural cross-section model of the wing. The analysis was performed on half of the wing to save analysis time and fall within the limits of our computational power. The current simulation mimics a cantilever beam thus the wing loading is applied at the tip of the wings which is occurring due to circulation.

Table 20: Structural Analysis Parameters

| S. No	Parameter	Value	Imperial Unit value
1	Mesh Element Size	15 mm	0.59 in
2	Wing Loading	5.650 kg/m^2	0.008 lb/in^2
3	Force	35.304 N	7.937 lbf
4	Force Convergence Criteria	Achieved	-
5	Total Deformation	6.2014 mm	0.244 in
6	Max Equivalent Elastic Strain	0.00455	-
7	Min Equivalent Elastic Strain	2.5 e-14	-
8	Max Equivalent Stress	26.734 MPa	3877.5 PSI
9	Min Equivalent Stress	3.05 e-11 MPa	4.436 e-9 PSI
10	Force Convergence Criteria	Achieved	-
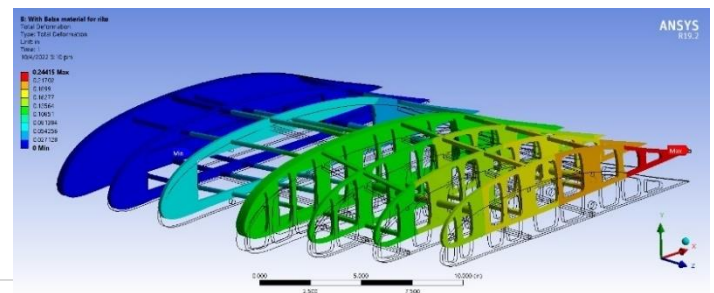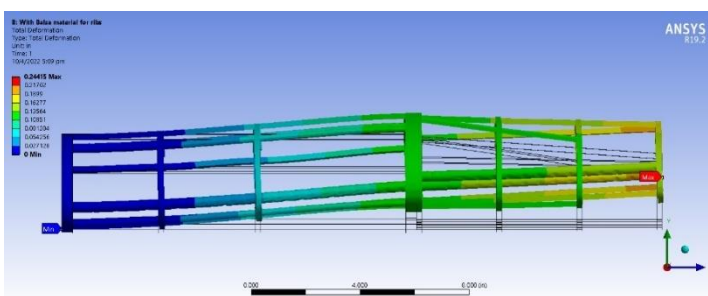
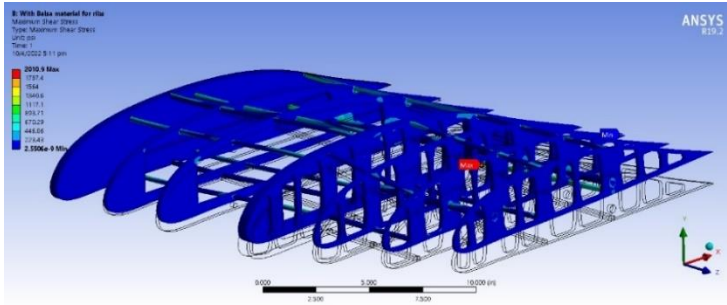
Figure 16: Total Deformation side and Iso Views
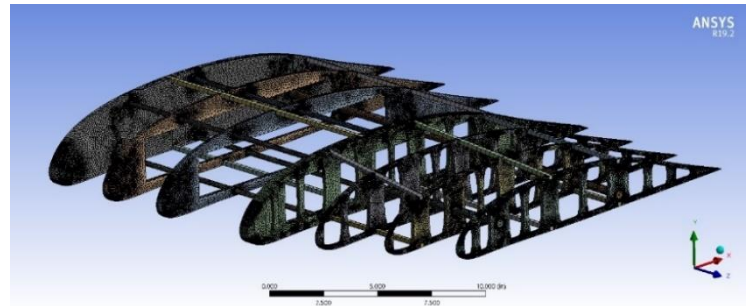
Figure 17: Maximum Shear Stress

Figure 18: Structural Mesh Iso view

11 Performance Prediction

The **MATLAB** software was also used to predict the behavior of aircraft in mid-air during the course of its flight to better understand the characteristics at various key points in the mission profile provided to us. Therefore, the aircraft was subjected to assumed gust forces so that a flight envelope could be plotted

Graph 10: Gust Envelope
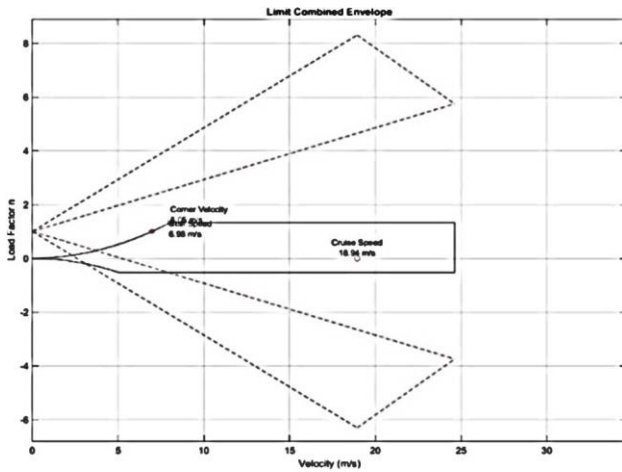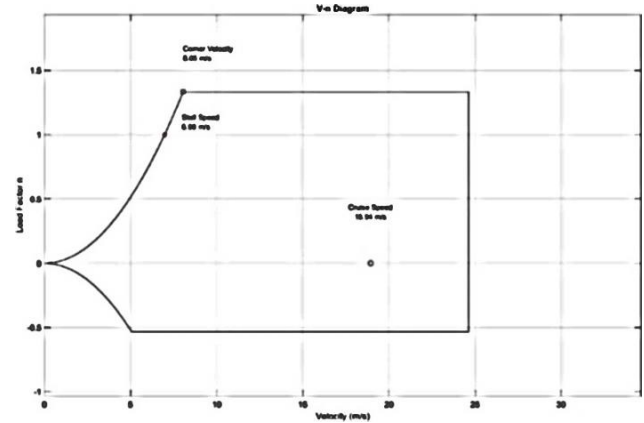

Graph 11: Limit Manoeuvre Envelope

Table 21: Performance Prediction

S. No	Parameter	Calculated Value	Value In Imperial Units
1	Take Off Velocity	7.39ms^{-1}	24.2 ft/s
2	Stall Velocity	6.98ms^{-1}	22.9 ft/s
3	Corner Speed	8.05ms^{-1}	26.4 ft/s
4	Cruise Speed	18.94ms^{-1}	62.1 ft/s

Max load factor calculated from **XFLR5** software was found to be n = 1.3018

C_{Lmax} was observed to be 1.833744 from the aircraft performance plots

The calculated propeller efficiency for our selected prop at 4.85lb of thrust and 10,000 **RPM** was found to be 0.7107

12 Fabrication and Testing

- A design layout is laid out on the paper in actual scale for placement of all the components in their specific positions,
- Ribs are designed and prepared to be cut using a laser cutting machine.
- The Carbon Fiber rods are used as spars and placed in the designated spot using the design layout.
- The material used to make wings, fuselage, and empennage is known as aeroply. We use polylactic
- acid to make a 3d print part which makes the joining of the fuselage to empennage possible.
- It can be printed at a low temperature and does not require a heated bed and strength ranges about 7,250 PSI.
- The grinding technique is used to cut aluminum bars/rods which we use in making of prototype.
- The sanding technique is used to increase the smoothness of parts.
- To join the parts, we use resins and hardeners to make an adhesive which makes better gluing.
- Drilling is a technique in which we use a drill bit to cut a hole of required cross sections in solid parts.
- Monokote is used to create a surface. Iron and heat gun is used to apply the covering film on the airframe surfaces.

Figure 19: Laser Cutting of Wing Ribs

Figure 20: Delivery Box Storage Location

Figure 21: Finished Prototype

13 Detailed CAD Design

The CAD models were designed in Solid Works, CATIA and Fusion 360 based on the complexity of the part.
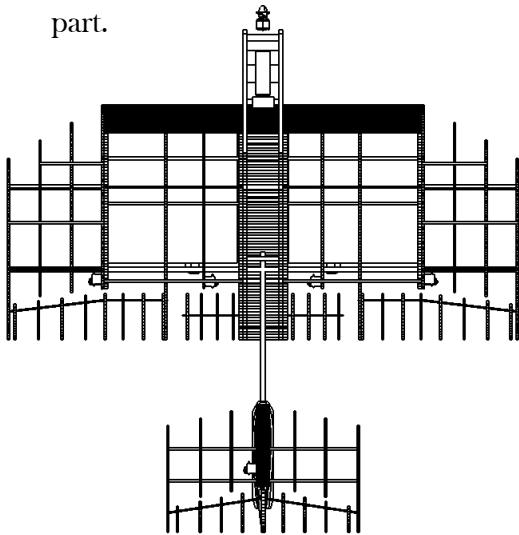

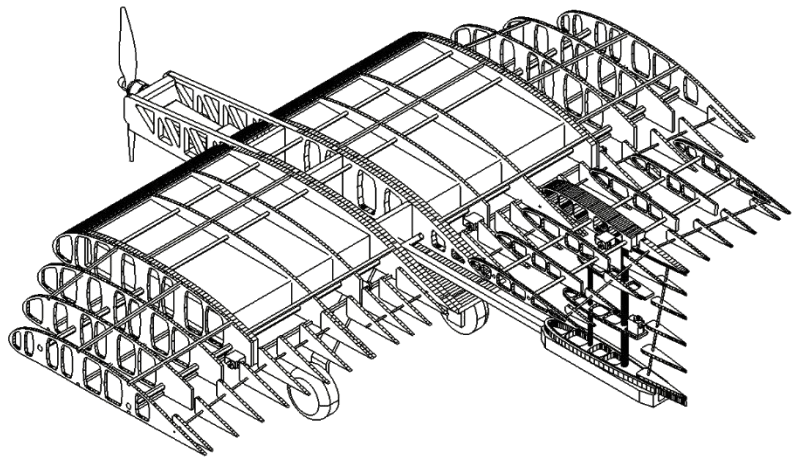Figure 22: 2D Top View Projection

Figure 23: 2D Iso view Projection
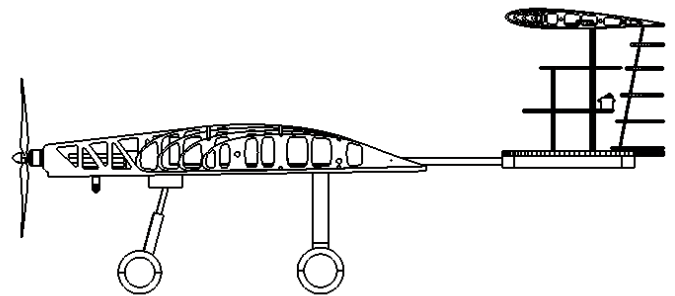

Figure 24: Box Retrieval Mechanism

Figure 25: 2D Side view Projection

Figure 26: Optimized Aircraft Iso view Render

14 Flight Test Validation

Table 22: Flight Test Validation

Attempt	Observation	Remark	Date
1	Tail vibrating vigorously	Tail Boom reinforcement needed	10th November 2021
2	Roll Stability compromised	Motor capacity and Wing tip separation need delaying	25th January 2022
3	Successful	All errors mitigated	26th March 2022

8 feet take off

Figure 27: Prototype Flight Tests

15 Acknowledgement

Special thanks to ANSYS, MATLAB and Solid Works for their generous sponsorship of their software licenses, without which this report and this project wouldn't be possible. Also, thanks to all the other open-source analysis platforms such as XFLR5, Wing Helper and Autodesk Fusion 360 for providing their software to us.

16 Innovations Summary

➢ Custom Designed Airfoil to accommodate the large boxes inside the wing.

➢ Embedded Fuselage design to minimize the mounting mechanism weight and give blended shape.

➢ Box retrieval mechanism through hinging of acrylic sheet at the wing's leading edge as shown in Section 13 .

17 Conclusion and Optimized Design

As the time progressed, the computational and analytical simulations of fluid flow and structural analysis were performed. Accordingly, prototypes were fabricated which led the design to take multiple turns to arrive at the current optimized configuration to meet all the requirements and constraints set by the SAE International for the Micro class competition along with achieving all the proposed ideas of the team as shown below:

Table 23: Optimised Design Table

Maximum Empty Weight	6.189 lb
Max Payload Lifting Capacity	2.011 lb
Payload Weight	1.000 lb (MS Steel plates)
Payload Bay Volume	1.5 x 1.5 x 2 cu.in
No. of large boxes	2
No. of Small boxes	0

18 References

[1] L. V. S. S. L. Varun and Y. D. Dwivedi, "Three-Dimensional Flow Analysis over Canard Configuration in Turbulence Model," *Grad. Res. Eng. Technol.*

[2] A. A. Khan, M. A. Ashraf, A. Shehzad, A. J. Qazi, and I. Hayat, "Computational and experimental studies of horizontal tail flutter suppression:" *https://doi.org/10.1177/0954410017725363*, vol. 233, no. 1, pp. 34–43, Aug. 2017, doi: 10.1177/0954410017725363.

[3] Vvsn. Bharadwaj, S. Ali, L. Farooq, and A. Ramesh, "A Effect of Elevator Deflection on Lift Coefficient Increment," *www.ijmer.com* /, vol. 5, no. 6, 2015, Accessed: Apr. 10, 2022. [Online]. Available: www.ijmer.com.

[4] K. Cunningham *et al.*, "Preliminary test results for stability and control characteristics of a generic t-tail transport airplane at high angle of attack," *AIAA Atmos. Flight Mech. Conf. 2018*, vol. 0, no. 209999, 2018, doi: 10.2514/6.2018-0529.

[5] A. Badis, "Subsonic Aircraft Wing Conceptual Design Synthesis and Analysis," *Int. J. Sci. Basic Appl. Res. Int. J. Sci. Basic Appl. Res.*, vol. 00, no. 1, pp. 0–00, 2017, Accessed: Apr. 10, 2022. [Online]. Available: http://gssrr.org/index.php?journal=JournalOfBasicAndApplied.

[6] İ. Halil Güzelbey, Y. Eraslan, and M. Hanifi Doğru, "Effects of Taper Ratio on Aircraft Wing Aerodynamic Parameters: A Comperative Study," *Eur. Mech. Sci.*, vol. 3, no. 1, pp. 18–23, Mar. 2019, doi: 10.26701/ems.487516.

[7] T. Ikeda, "Aerodynamic Analysis of a Blended-Wing-Body Aircraft Configuration," RMIT University, Melbourne, Australia , 2006.

[8] W. P. Nelms, "Assessment of Aerodynamic Performance of V/STOL and STOVL Fighter Aircraft," *Nasa*, no. April, 1984.

[9]   HWANG Younghee, "제2언어습득환경에 따른 제2언어보존의 유형 －한국노년층일본어의 변이형을 대상으로－," *J. japanese Lang. Cult.*, vol. null, no. 14, pp. 279–298, 2009, doi: 10.17314/jjlc.2009..14.014.

[10]   C. L. Sánchez, D. S. Franco, and R. C. Munjulury, "Hurricane-CS: Control surfaces and high lift devices modeling and sizing program," *31st Congr. Int. Counc. Aeronaut. Sci. ICAS 2018*, pp. 1–10, 2018.

[11]   J. H. Diekmann, "Flight Mechanical Challenges of STOL Aircraft Using Active High-Lift."

[12]   "Aircraft Design Project Design of 100 Seater STOL Commuter Aircraft." https://www.researchgate.net/publication/340933545_Aircraft_Design_Project_Detail

[13]   T. Ema, "An experimental study of pilots' control characteristics for flight of an STOL aircraft in backside of drag curve at approach and landing," *Ergonomics*, vol. 35, no. 5–6, pp. 541–550, 1992, doi: 10.1080/00140139208967835.

[14]   S. ANDERSON, "An overview of V/STOL aircraft development," Oct. 1983, doi: 10.2514/6.1983-2491.

[15]   O. E. Nahum, Y. Hadas, and A. Kalish, "A Combined Freight and Passenger Planes Cargo Allocation Model," *Transp. Res. Procedia*, vol. 37, pp. 354–361, Jan. 2019, doi: 10.1016/J.TRPRO.2018.12.203.

[16]   "THE EFFECT OF ASPECT RATIO ON AERODYNAMIC PERFORMANCE AND FLOW SEPARATION BEHAVIOR OF A MODEL WING COMPOSED FROM DIFFERENT PROFILES." https://www.resea

[17]   Y. D. Dwivedi and L. Lohitasya Varun, "Aerodynamic Characterization Of Albatross-Inspired Airfoils/Wings," *Int. J. Adv. Sci. Technol.*, vol. 29, n

[18]   R. E. M. Nasir, W. Kuntjoro, and W. Wisnoe, "Aerodynamic, Stability and Flying Quality Evaluation on a Small Blended Wing-body Aircraft with Canard Foreplanes," *Procedia Technol.*, vol. 15, pp. 783–791, Jan. 2014, doi: 10.1016/J.PROTCY.2014.09.051.

[19]   "Aircraft Design: A Systems Engineering Approach Mohammad H. Sadraey

[20]   C. Humphreys-Jennings, I. Lappas, and D. M. Sovar, "Conceptual design, flying, and handling qualities assessment of a blended wing body (BWB) aircraft by using an engineering flight simulator," *Aerospace*, vol. 7, no. 5, 2020, doi: 10.3390/AEROSPACE7050051.

[21]   P. Panagiotou, E. Giannakis, G. Savaidis, and K. Yakinthos, "Aerodynamic and structural design for the development of a MALE UAV," *Aircr. Eng. Aerosp. Technol.*, vol. 90, no. 7, pp. 1077–1087, 2018, doi: 10.1108/aeat-01-2017-0031.

[22]   S. Tsach, A. Peled, D. Penn, B. Keshales, and R. Guedj, "Development trends for next generation UAV systems," *Collect. Tech. Pap. - 2007 AIAA InfoTech Aerosp. Conf.*, vol. 1, no. May, pp. 490–503, 2007, doi: 10.2514/6.2007-2762.

[23]   L. Gs, P. Balmuralidharan, G. Sankar, K. Selvaraj, N. Balachandran, and A. Division, "High Lift Two-Element Airfoil Design for MALE UAV Using CFD," *20th Annu. CFD Symp.*, no. August, 2018.

[24]   K. Jayakrishna, V. R. Kar, M. T. H. Sultan, and M. Rajesh, *Materials selection for aerospace components*, no. July 2019. Elsevier Ltd, 2018.

[25]   P. Panagiotou, S. Fotiadis-Karras, and K. Yakinthos, "Conceptual design of a Blended Wing Body MALE UAV," *Aerosp. Sci. Technol.*, vol. 73, pp. 32–47, 2018, doi: 10.1016/j.ast.2017.11.032.
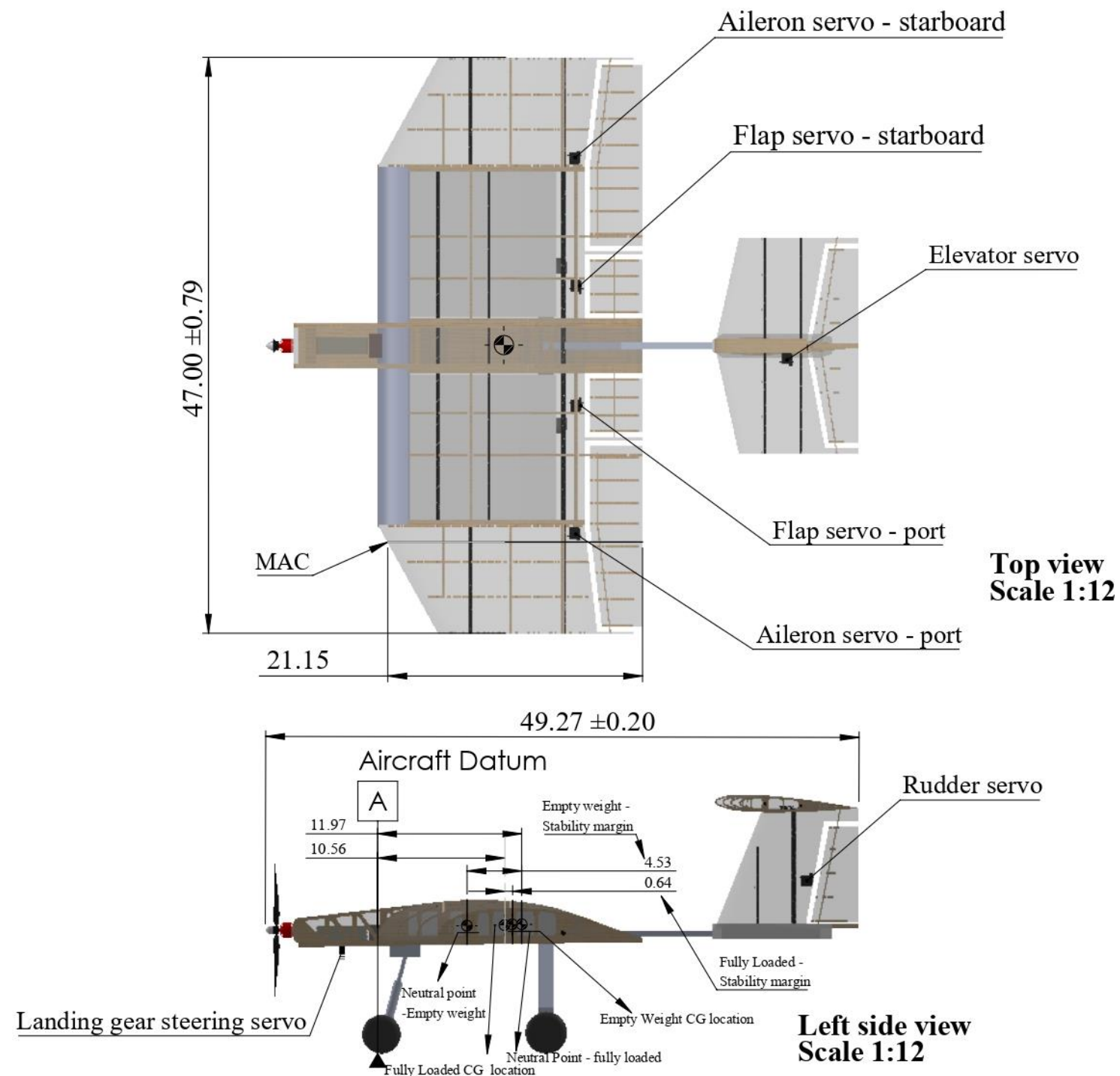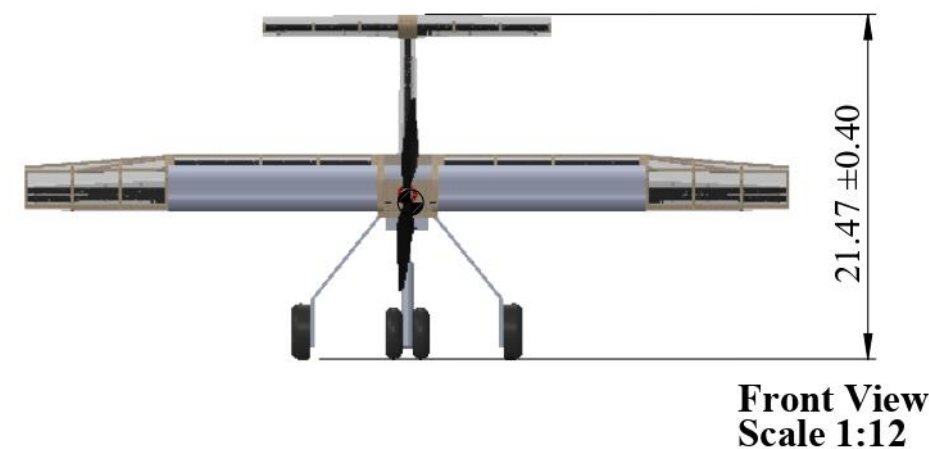
WEIGHT AND BALANCE TABLE

Component Name	Distance from datum (in)	Force (lbf)	Resultant Moment (lbf-in)
Propeller	-8.468	0.101	-0.857
Motor	-8.662	0.306	-2.655
Boom	25.750	0.168	4.315
Tail mount	32.796	0.272	8.920
Fin	33.959	0.203	6.907
Fuselage	6.412	0.596	3.821
Tail	33.449	0.375	12.543
Wing	9.738	1.546	15.055
Landing gear	7.966	1.090	8.682
Payload	0.000	1.000	0.000
Battery	-2.980	0.342	-1.018
Delivery Box-port	8.698	0.375	3.260
Delivery Box-starboard	8.698	0.375	3.260
Landing gear servo	-3.000	0.030	-0.089
Aileron servo - port	16.340	0.030	0.483
Aileron servo - starboard	16.340	0.030	0.483
Flap servo - port	16.520	0.030	0.488
Flap servo - starboard	16.520	0.030	0.488
Elevator servo	33.987	0.030	1.004
Rudder servo	35.679	0.030	1.054
ESC	-2.864	0.139	-0.398
Power Limiter	-2.910	0.040	-0.115
Receiver	-2.631	0.033	-0.086

Top view — Scale 1:12

Aileron servo - starboard
Flap servo - starboard
Elevator servo
Flap servo - port
Aileron servo - port
MAC
47.00 ±0.79
21.15

Left side view — Scale 1:12

49.27 ±0.20
Aircraft Datum
A
11.97
10.56
Empty weight - Stability margin
4.53
0.64
Rudder servo
Neutral point - Empty weight
Fully Loaded - Stability margin
Empty Weight CG location
Neutral Point - fully loaded
Fully Loaded CG location
Landing gear steering servo

Front View — Scale 1:12

21.47 ±0.40

All dimensions are in inches

Wingspan	47 inches
Mean Aerodynamic Chord(MAC)	21.151 inches
Empty weight	6.189 lbs
Battery capacity	1500 mAh
Motor make and model	T - Motor AT 2820 Long Shaft
Motor KV	880
Propeller manufacturer	APC
Propeller diameter and pitch	12 inches diameter, 6 inch pitch
Servo manufacturer and model number	TowerPro MG90S
Servo torque	24.99 oz-in (at 4.8V)

|	
TEAM NAME	IARE LAKSHYA
TEAM NUMBER	312
SCHOOL NAME	INSTITUTE OF AERONAUTICAL ENGINEERING
SCALE: 1:12	SAE AERO DESIGN EAST
SIZE: ANSI B	MICRO CLASS

SHEET 1 OF 1

20 Appendix B : Tech Data Sheet – Aircraft Performance Prediction

The following aircraft performance prediction graphs were plotted in MATLAB using the real time data from other sources.

Graph 12: Ground Distance Prediction plot
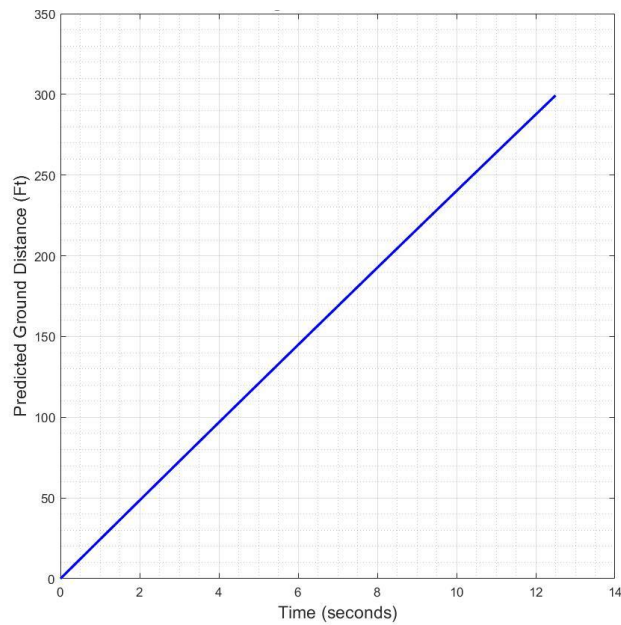
Graph 13: Altitude Prediction Plot